



Global Journal of Engineering Science and Research Management

EQUILIBRIUM AND KINETIC MODELING OF ADSORPTION OF DISPERSE BLUE 79 ONTO DIFFERENT ADSORBENTS

M. Joudi, H. Hafdi, J. Mouldar, H. Nasrellah, M.A. El Mhammedi, M. Bakasse*

* Laboratoire de Chimie Organique Bioorganique et Environnement, Faculté de Sciences, Université Chouaib Doukkali Morocco
Univ Hassan I, Laboratoire de Chimie et Modélisation Mathématique, Faculté Polydisciplinaire, 25000 Khouribga, Morocco

DOI: 10.5281/zenodo.805427

KEYWORDS: Adsorption; Disperse Blue 79; Chitosan; Phosphogypsum; Natural Phosphate; Isotherm models.

ABSTRACT

Azo dyes are generally used in food, cosmetic, textile, pharmaceutical, and leather industries. Many of these dyes are carcinogens and need a treatment. The aim of the present study was to use chitosan (CHT), phosphogypsum (PG) and natural phosphate (NP) powders for the removal of Disperse Blue 79 (DB 79) from aqueous solution. The effects of contact time, initial dye concentration, adsorbents doses, solution pH, and temperature on the batch adsorption process were systematically studied. Isotherm models were applied to the experimental equilibrium data and pseudo-first order, pseudo-second order kinetic models were used to describe the kinetic data and to evaluate the rate constants. The thermodynamic parameters, such as the changes in enthalpy, entropy, and Gibbs free energy were also studied. The results show that the chitosan, phosphogypsum and natural phosphate could be used for the removal of DB 79 in wastewater treatment.

INTRODUCTION

Dyes represent an important class of organic pollutants, which are generally used for coloring products in textile industries. Azo dyes are widely used in many industries, especially the disperse azo dyes [1]. Disperse dyes have an aromatic moieties linked together by azo ($-N-N-$) chromospheres and have been used in the textile industry [2]; these dyes are not degraded during conventional treatment of industrial effluents and need to be treated. To treat the dyeing wastewater, a number of methods including adsorption [3], ozonation [4] and coagulation-flocculation [5] have been investigated.

The adsorption process is an effective method to remove pollutants from wastewater. To save the environment, the adsorbents based on biopolymers such as cellulose [6], alginate [7] and chitosan [8], composites [9] and clay [10], etc. as adsorbents for the removal of dyes from wastewater.

Chitosan and natural phosphate are abundant and low-cost adsorbents in the world [11, 12], phosphogypsum [13] is a by-product of production of phosphoric acid, which is produced in large quantities worldwide.

In this study, chitosan, phosphogypsum and natural phosphate powders were characterized and the adsorption behavior of DB 79 by different adsorbents was investigated. Kinetics, isotherms and thermodynamic parameters of adsorption process were calculated.

MATERIALS AND METHODS

Chemical and physical properties of different adsorbents

The chitosan was purchased from sigma-Aldrich the product number is 419419, the treated NP was obtained from khouribga region and has the following chemical composition: CaO (54.12%), P₂O₅ (34.24%), F⁻ (3.37%), SiO₂ (2.42%), SO₃ (2.21%), CO₂ (1.13%), Na₂O (0.92%), MgO (0.68%), Al₂O₃ (0.46%), Fe₂O₃ (0.36%), K₂O (0.04%) and diverse metals in the range of ppm, PG was obtained from phosphate industries and the chemical composition was CaO (32.27%), P₂O₅ (0.93%), F⁻ (0.12%), SiO₂ (0.55%), SO₃ (45.1%), Na₂O (0.14%), MgO (0.16%), Al₂O₃ (0.14%), Fe₂O₃ (0.83%), K₂O (0.18%).

**Test chemicals and analysis**

Disperse Blue DB 79 (DB 79) was purchased from sigma-Aldrich the product number is 12239-34-8 and used without any further purification. The chemical structure of DB 79 is shown in Figure 1. The initial pH was adjusted with NaOH or HCl solutions. All of the reagents were analytical reagent grade.

A stock solution of 100 mg.L⁻¹ was prepared by dissolving exactly 100 mg of DB 79 in 1000 mL distilled water. The desirable experimental concentrations of solutions were prepared by diluting the stock solution with distilled water.

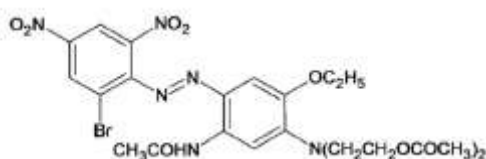


Figure 1: Molecular structures of disperse blue 79.

Adsorption experiments

Kinetic adsorption experiments of DB 79 were carried out in batch process in the presence of specific amounts of CHT, PG and NP in 100 mL solution by varying the DB 79 concentration (20, 50, 70 and 100 mg.L⁻¹) and adsorbent dose from 0.1 to 1g.L⁻¹ for CHT, 1 to 15g.L⁻¹ for PG and NP. Samples were then collected at different time intervals and the left out concentration in the clear centrifugation supernatant solution was analyzed using Jasco V-630 UV visible spectrophotometer at $\lambda_{max}=537$ nm of DB 79. The effect of pH on the removal amount of DB 79 was analyzed over the pH range from 4 to 10, whereby adjustment was made using 0.1 N NaOH and 0.1 N HCl solutions. The experiments were also conducted at different temperatures, 293, 303, 313, 323 and 333 K, while agitation was provided for 135 min for CHT, PG and 240 for NP using velp scientifica AG 460, which was sufficient to reach equilibrium.

The adsorption percentage (%R) and adsorption capacity values at equilibrium q_e mg.g⁻¹ and time q_t (mg.g⁻¹) were calculated using the following equations:

$$\%R = \frac{C_0 - C_e}{C_0} \times 100 \quad (1)$$

$$q_e = \frac{C_0 - C_e}{W} \times V \quad (2)$$

$$q_t = \frac{C_0 - C_t}{W} \times V \quad (3)$$

Where C_t is the dye concentration at time (t), C_0 (mg.L⁻¹) is the initial dye concentration, C_e is the dye concentration at equilibrium, V (l) is the volume and W (g) is the amount of the adsorbent in the solution.

RESULTS AND DISCUSSION**Characterizations of CHT, PG and NP**

The surface functional groups of CHT, PG and NP were identified using an FT-IR spectrometer (Alpha Burker). The FT-IR spectra of the samples were then analyzed at a range of 400–4000cm⁻¹. The X-ray diffraction (XRD) using X'Pert Pro (PANalytical) produced at 45 kV and 40 mA. The diffraction angles (2θ) were scanned between 6° and 60°.

FT-IR spectroscopy

Figure 2 exhibits the IR of CHT, PG and NP. The spectrum of CHT presented in figure. 2.a is composed of several characteristic peaks. The spectrum shows a peak at 3363 cm⁻¹ that was assigned to O–H stretching band and N–H stretching bands appear at 3284 cm⁻¹. The characteristic bands of C–O–C linkage were observed at 1150 and 1034 cm⁻¹. Finally, the C–N band appears at 898 cm⁻¹ [14].



Global Journal of Engineering Science and Research Management

The spectra obtained for the phosphogypsum is shown in figure. 2.b. The IR spectrum of phosphogypsum has an intense peak around 1100 cm^{-1} . The PG has an additional two weak bands at 650 cm^{-1} and at 2300 cm^{-1} corresponding of sulfate groups. The PG has also two bands characteristic of H_2O at 3500 cm^{-1} and 1500 cm^{-1} [15].

The IR absorption spectrum (Figure 2.c) shows band characteristics of NP. The bands located between 1455 and 1430 cm^{-1} . The spectrum of IR shows also the bands of phosphates, bands located between 780 and 800 cm^{-1} which could appear from the vibration of the silicate groups [16].

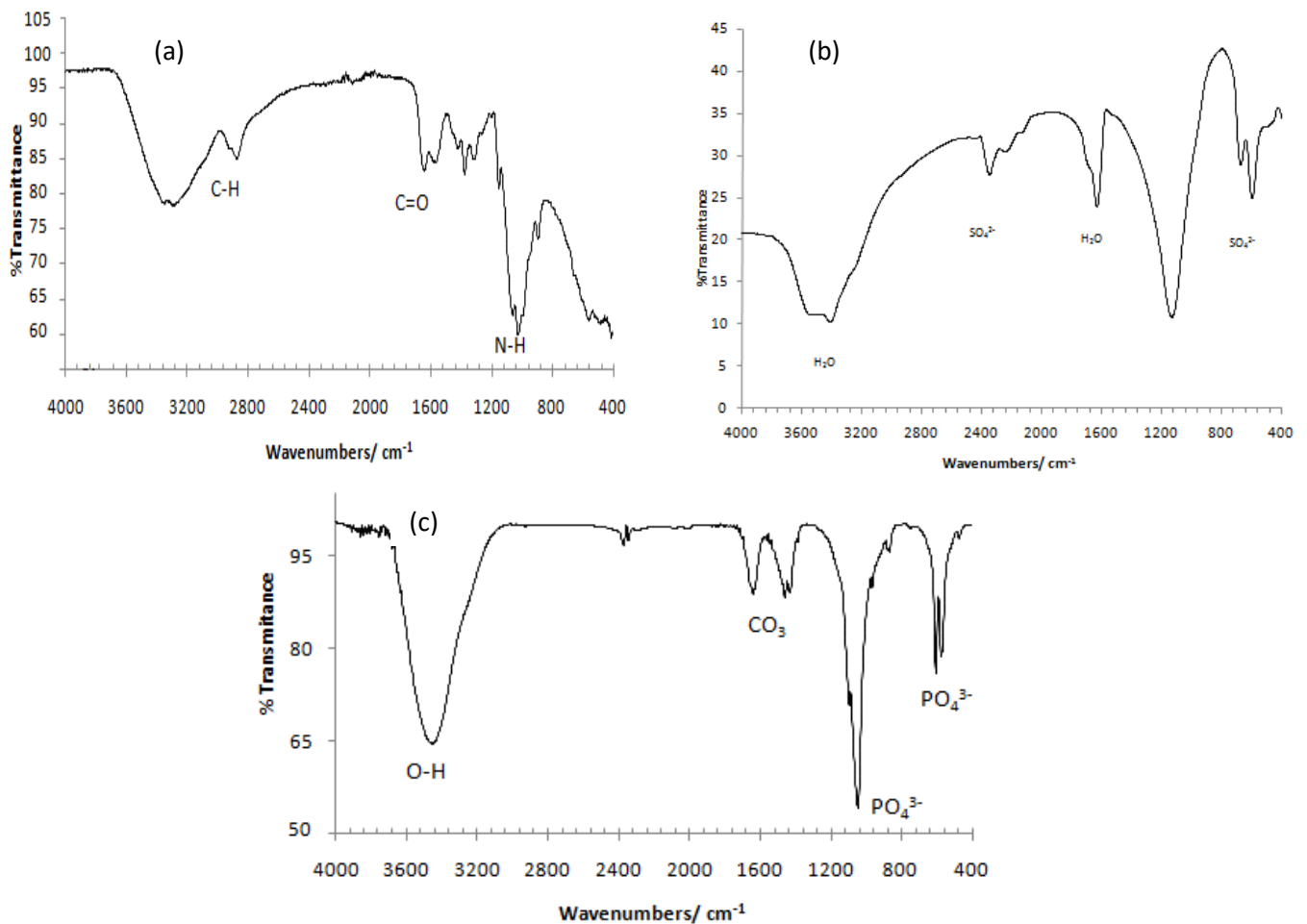


Figure 2 FT-IR patterns of (a) chitosan, (b) phosphogypsum and (c) natural phosphate.

X-ray powder diffraction:

The spectrum of CHT (Figure 3a) showed two peaks, one at $2\theta = 10^\circ$ and another at $2\theta = 21^\circ$ which were assigned to (020) and (110) [17].

The X-ray spectrum of the PG was presented in Figure 3.b. The PG was identified to the dihydrated calcium sulfate $\text{CaSO}_4 \cdot 2\text{H}_2\text{O}$ [18]. Figure 3.c shows the patterns of X-ray diffraction of NP. The peaks that correspond to the SiO_2 structure appears around $2\theta = 26^\circ$ and $2\theta = 35^\circ$ characterized by diffraction planes (002) and (202). The peak characteristic of CaF_2 appears at 30.2° . The Figure 3.c shows also that the structure of NP is similar to that of fluorapatite ($\text{Ca}_{10}(\text{PO}_4)_6\text{F}_2$) [19].

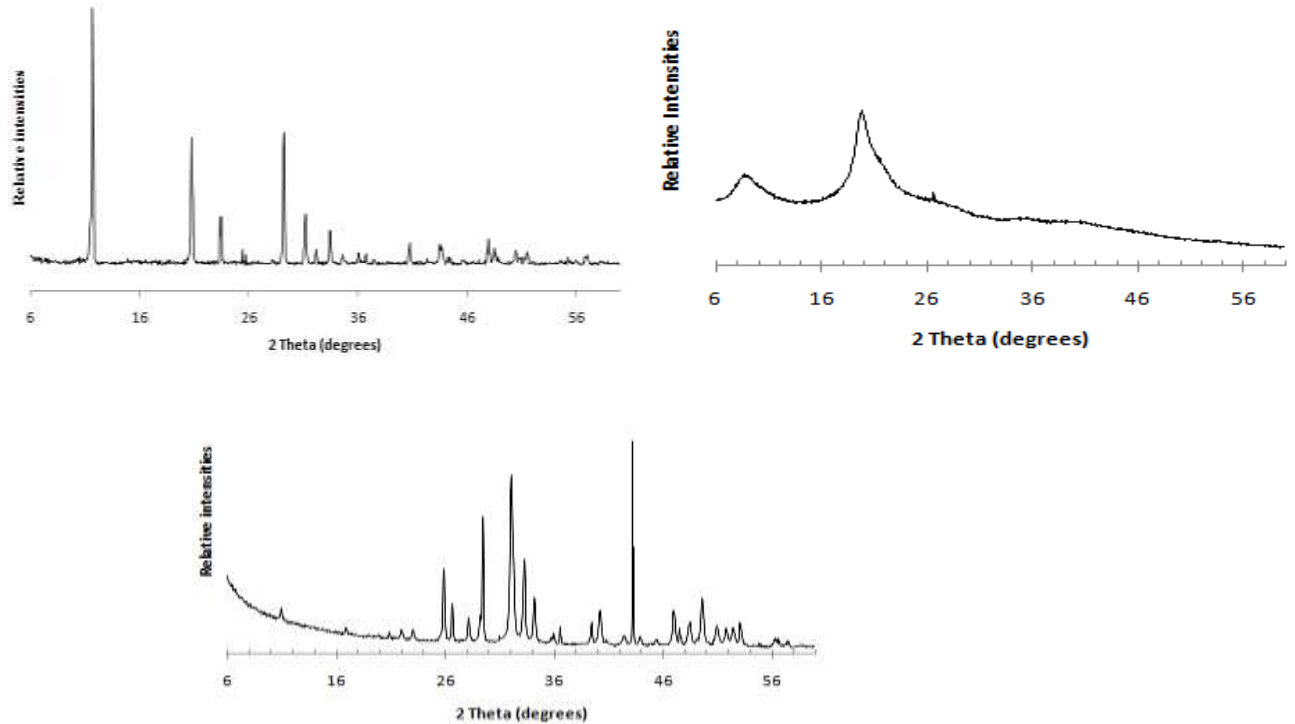
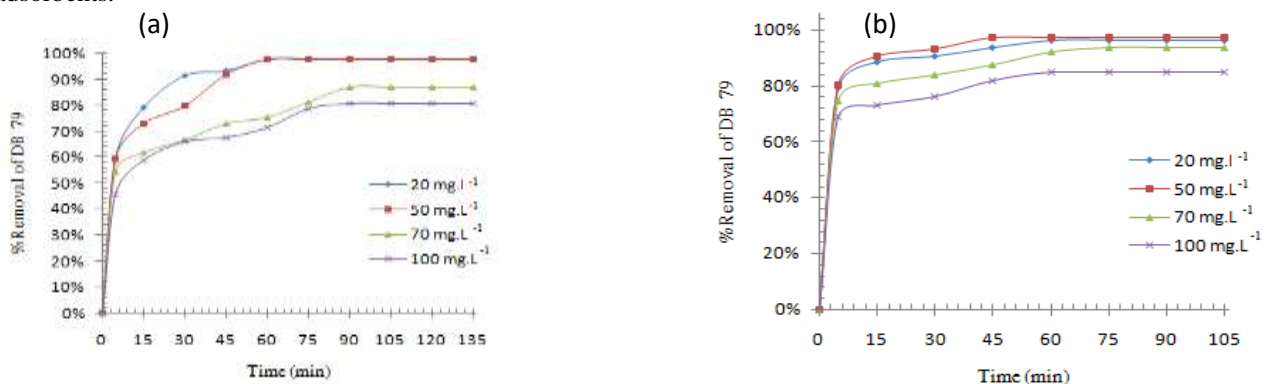


Figure 3. XRD patterns of (a) chitosan, (b) phosphogypsum and (c) natural phosphate.

Effect of concentration and contact time

The effect of contact time on DB 79 adsorption by CHT, PG and NP was investigated at different initial concentrations of DB 79. As it can be seen in Figure 4, the adsorption of DB 79 was fast at the initial stage, and then, it became slower near the equilibrium. The optimum contact time was found to be 60 min in the case of chitosan and PG and 180 min for NP.

The percentage of DB 79 removal decreased with increasing initial dye concentration for all adsorbents. The decrease of DB 79 adsorption rate is perhaps due to the slow pore diffusion of the dye ions into the bulk of adsorbents.



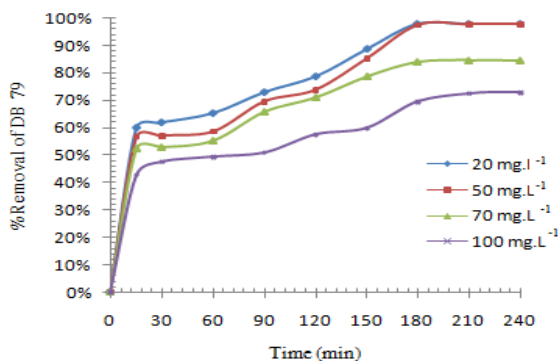


Figure 4. Effect of contact time and initial dye concentration on the adsorption of DB 79 onto (a) CHT, (b) PG and (c) NP

Effect of adsorbent dosage

In order to find the optimum dose of each adsorbent for maximizing the interactions between DB 79 molecules and adsorption sites of different adsorbents in the solution, various amounts of CHT (0.1- 1 g.L⁻¹), PG and NP (1- 15 g.L⁻¹) were varied.

Figure 5 presents the effects of CHT, PG and NP dosages on the adsorption of DB79. It was observed that initially, the removal percentage of DB 79 increased rapidly with the increase in adsorbents doses, after the critical dose, the removal percentage almost reached a constant value. The increase in DB 79 removal percentage was due to increased available sorption surface and the availability of more adsorption sites [20].

Therefore, 0.5 g.L⁻¹ of CHT, 10 g.L⁻¹ of PG and 7 g.L⁻¹ of NP were chosen for further studies on DB 79 removal.

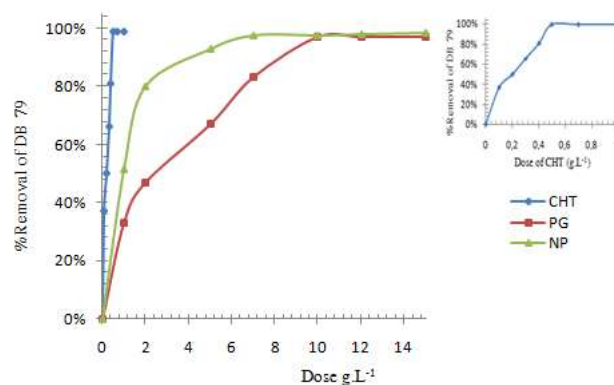


Figure 5. Effect of adsorbent dose on the adsorption of DB 79 by CHT, PG and NP (experimental conditions: initial dye concentration: 50mg.L⁻¹, temperature: 293 K, contact time: 60 min for CHT, PG and 180 min for NP).

Effect of pH

The influence of pH on adsorption of DB 79 is shown in Figure 6. For the three adsorbents the maximum removal was achieved at pH ranging from 4 to 8. While the pH increased from 8 to 10, the removal of DB79 decreased to 81%, 90% and 95%, for CHT, PG and NP respectively. Such phenomena, is maybe due to the decomposition of the azo group in disperse dye molecules because the azo group is unstable in higher pH [21] for this reason, at pH alkaline, more dye chromospheres were damaged, leading to a decrease in the adsorption removal by the different adsorbents.

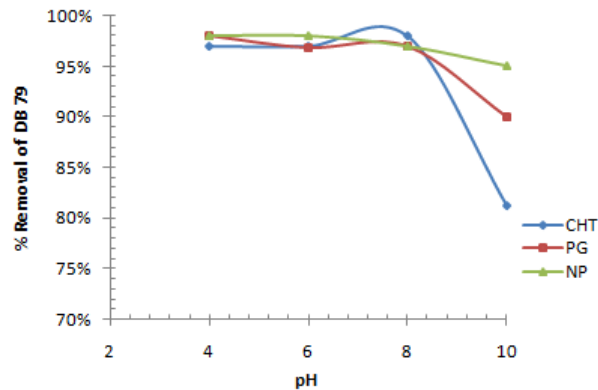


Figure 6. Effect of pH on the adsorption of DB 79 by CHT, PG and NP (experimental conditions: initial dye concentration: $50\text{mg}\cdot\text{L}^{-1}$, temperature: 293 K, contact time: 60 min for CHT, PG and 180 min for NP)

Effect of temperature

Adsorption studies were carried out at five different temperatures (293, 303, 313, 323 and 333 K). The experimental results showed that the removal of DB 79 using CHT decreased with the increase in temperature (figure 7 a), indicating the exothermic nature of the adsorption reaction of DB 79 onto chitosan. The decrease in the rate of adsorption with the increase in temperature may be due to the affinity of DB 79 to escape from the solid phase to bulk phase [22]. The removal of DB 79 by PG and NP increases with increasing temperature. The rise in removal of DB 79 with increasing temperature is due to the fact that the reaction rate between DB 79 and the surface of the NP and PG increases with temperature. This suggests that the interaction between the adsorbate and the adsorbent is endothermic in nature [23].

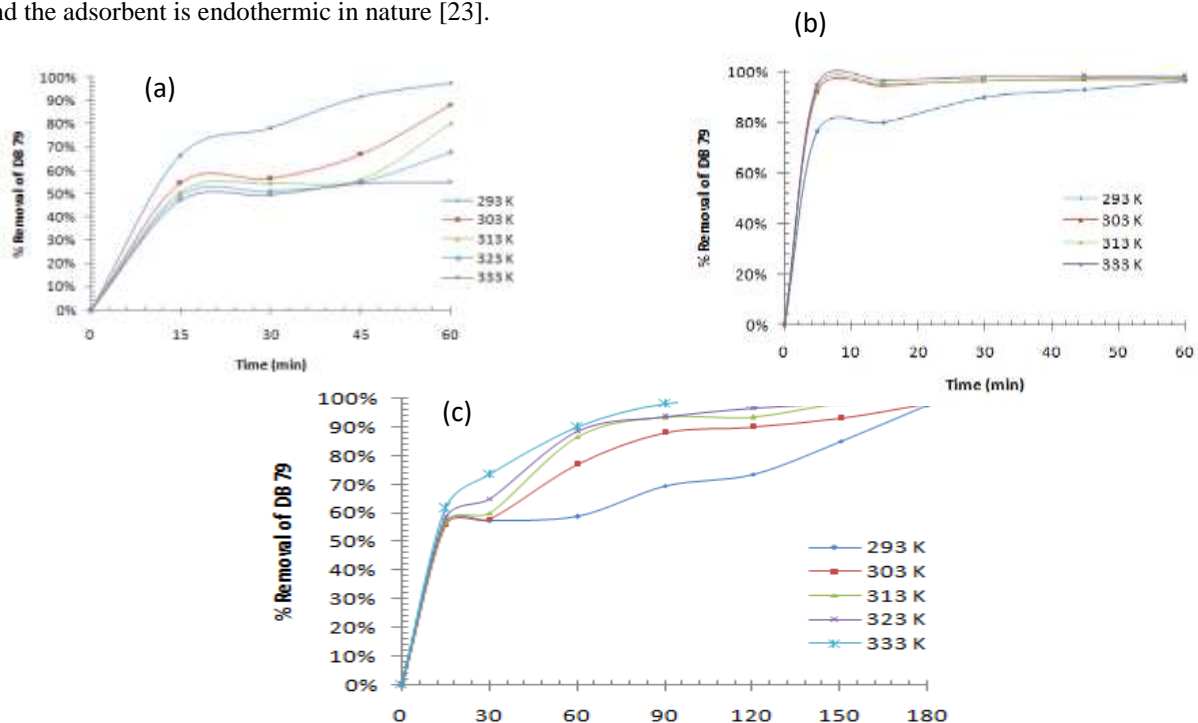


Figure 7: Effect of temperature on DB 79 removal by (a) CHT, (b) PG and (c) NP

Evaluation of adsorption kinetics

In order to determine the kinetic parameters of DB 79 removal by CHT, PG and NP, the kinetic models including the pseudo-first-order and the pseudo-second-order were applied to evaluate the experimental data. The pseudo-first order equation can be expressed as follows [24]:



$$\log(q_e - q_t) = \log q_e - \frac{k_1}{2.303} t \quad (4)$$

Where k_1 (min^{-1}) is the rate constant of the adsorption process, while q_e and q_t are the adsorption capacities at equilibrium, and at time t (min). The values of q_e and k_1 were determined from the intercepts and the slope of the plot of $\log(q_e - q_t)$ versus t .

The rate equation for pseudo-second-order model [25] is given by:

$$\frac{t}{q_t} = \frac{1}{k_2 q_e^2} + \frac{t}{q_e} \quad (5)$$

Where q_e and q_t are the adsorption capacities at equilibrium, and at time t (min), while k_2 ($\text{g} \cdot \text{mg}^{-1} \cdot \text{min}^{-1}$) is the rate constant of second-order adsorption.

The kinetic parameters from the pseudo-first and the pseudo-second order models were calculated and listed in Table 1. The plots of pseudo-first-order and pseudo-second-order kinetics models are shown in Figure 8 I and II. The results indicate that the pseudo-second order model fits the experimental data of DB 79 removal for all adsorbents, since all of their correlation coefficient (R^2) values are beyond 0.995.

The values of Q_e calculated by the pseudo-second-order model showed a good agreement with the experimental values ($q_{e, \text{exp}}$). But, the values of Q_e calculated obtained from the pseudo-first order model do not give reasonable values. These results suggested that the pseudo-second-order adsorption mechanism was predominant for the adsorption of DB 79 onto CHT, PG and NP in this study.

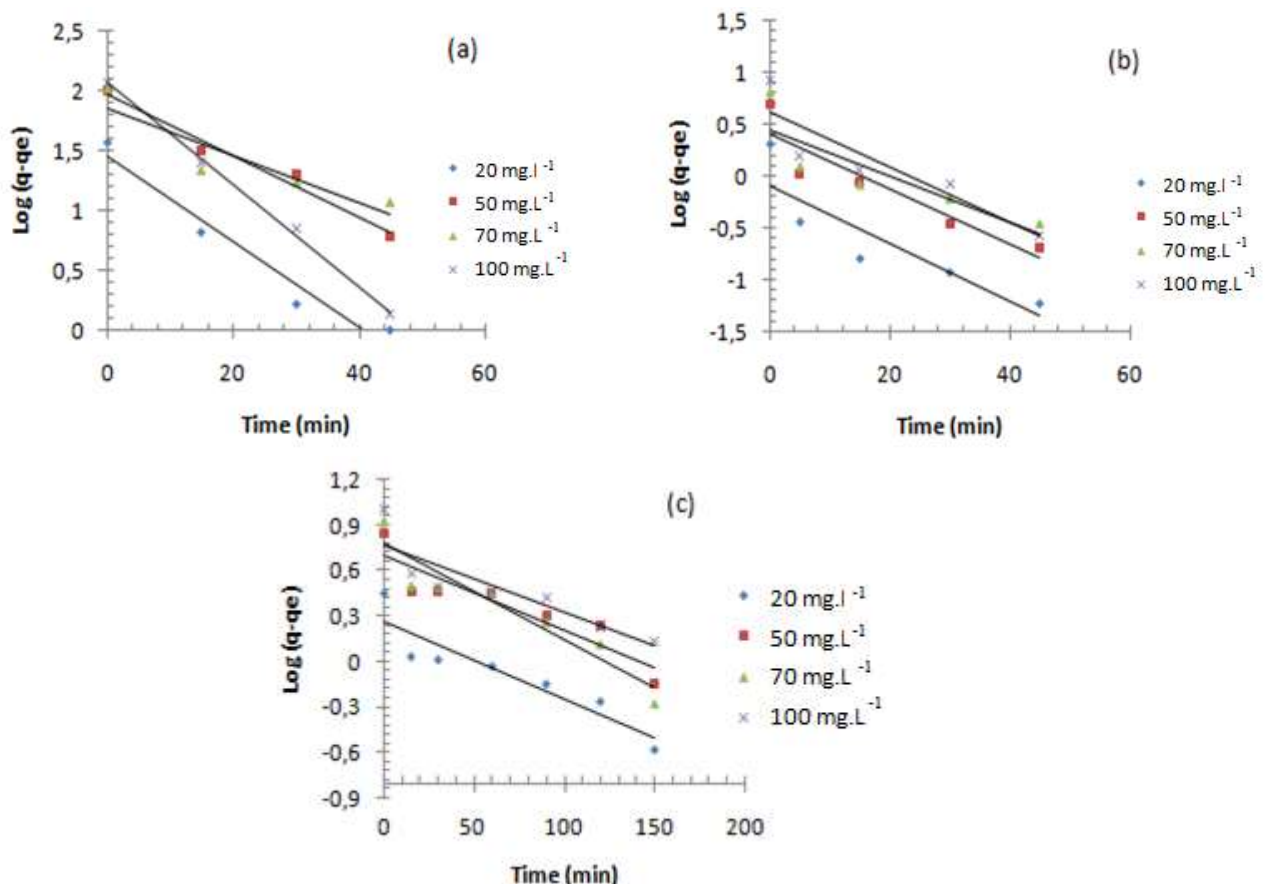


Figure 8.I: Pseudo-first-order plots for adsorption of DB 79 onto (a) CHT, (b) PG and (c) NP.

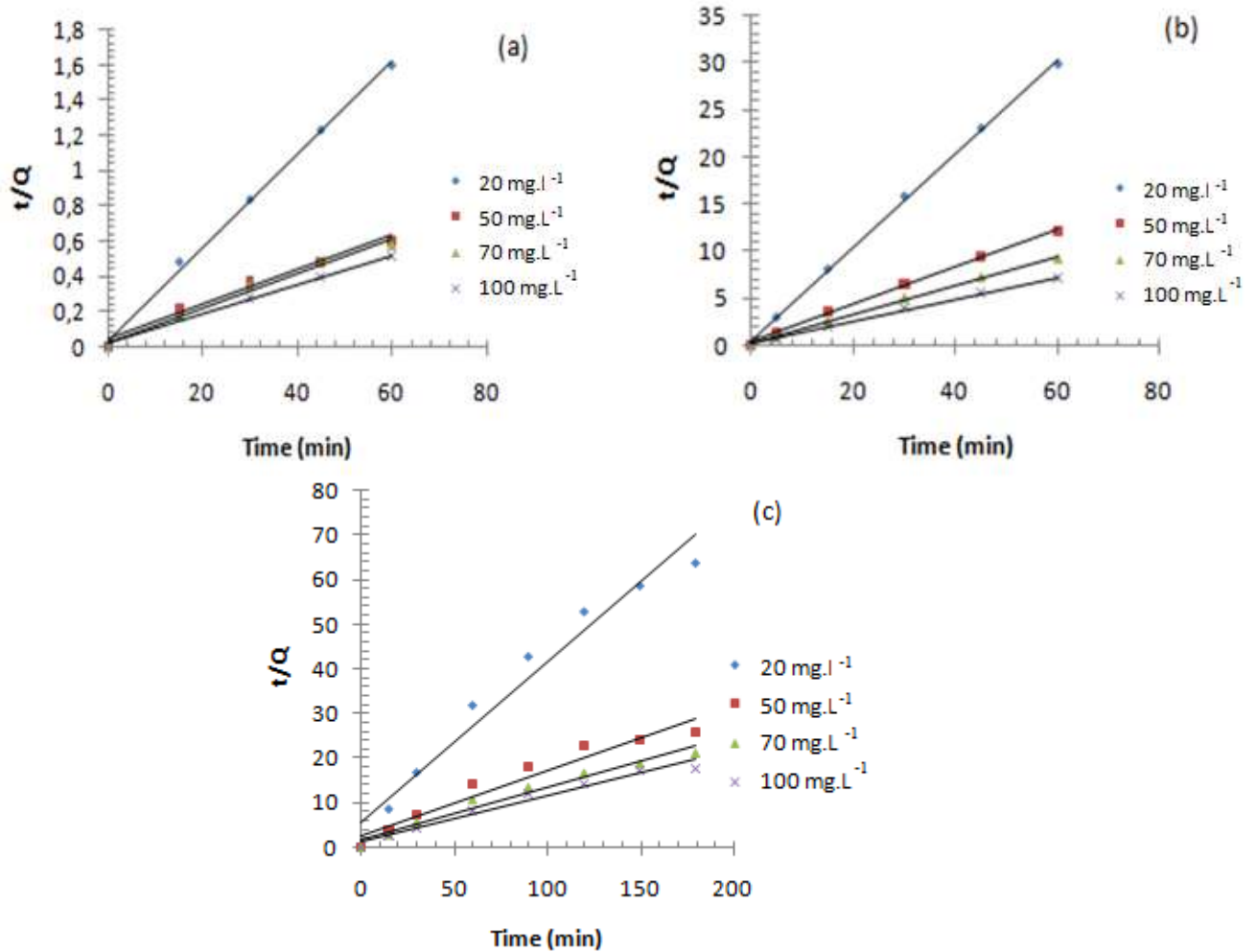


Figure 8.II: Pseudo-second-order plots for adsorption of DB 79 onto (a) CHT, (b) PG and (c) NP.

Table 1 : Kinetic parameters for the adsorption of DB 79 onto CHT, PG and NP.

Adsorbent	C (mg.L ⁻¹)	Q _{exp}	pseudo-First ordre			pseudo-seconde ordre		
			Q _{calcul}	K	R ²	Q _{calcul}	K	R ²
CHT	20	37.50	28.12	0.08	0.949	38.46	0.02	0.997
	50	99.17	93.97	0.06	0.976	111.11	0.002	0.975
	70	103.83	71.78	0.04	0.83	111.11	0.00	0.99
	100	116.83	116.950	0.097	0.997	125.000	0.004	0.994
PG	20	2.01	0.822	0.064	0.785	2.012	0.520	0.999
	50	4.93	0.398	0.060	0.785	4.975	0.126	0.997
	70	6.50	2.844	0.051	0.742	6.494	0.113	0.997
	100	8.44	4.121	0.060	0.822	8.475	0.080	0.996
NP	20	2.82	1.866	0.012	0.858	2.786	0.023	0.964
	50	7.02	5.000	0.009	0.840	6.944	0.008	0.942
	70	8.47	5.943	0.014	0.891	8.621	0.008	0.970



	100	10.10	5.929	0.009	0.798	9.804	0.008	0.970
--	-----	-------	-------	-------	-------	-------	-------	-------

Adsorption isotherms

The Langmuir isotherm supposed that a monomolecular layer is created when adsorption takes place without any interaction between the adsorbed molecules and the adsorbent [26]. It is used to evaluate maximum dye adsorption capacity. The Langmuir equation is represented as (Eq. (6)):

$$\frac{C_e}{q_e} = \frac{1}{K_L q_m} + \frac{1}{q_m} C_e \quad (6)$$

Where q_m and q_e (mg.g^{-1}) are the maximum and equilibrium adsorption capacity, respectively, C_e is the equilibrium concentrations of dye solution (mg.L^{-1}) and K_L (L.mg^{-1}) is the Langmuir adsorption constant related to the energy of adsorption. The essential characteristics of the Langmuir isotherm can be expressed by means of R_L a dimensionless constant separation factor [27], The R_L is defined as: (7)

$$R_L = 1 / (1 + K_L C_0) \quad (7)$$

Where C_0 (mg L^{-1}) is the highest initial concentration of adsorbent, and K_L (L.mg^{-1}) is the Langmuir constant. The parameter R_L indicates the type of adsorption:

The adsorption is unfavorable when $R_L > 1$, favorable when $0 < R_L < 1$, irreversible when $R_L = 0$ and when $R_L = 1$, the adsorption is linear.

The Freundlich isotherm is a special model for heterogeneous surface energy of adsorption [28]. The Freundlich isotherm can be described as:

$$q_e = K_F C_e^{1/n} \quad (8)$$

Where q_e is the amount of adsorbate adsorbed at equilibrium (mg.g^{-1}), C_e is the equilibrium concentration of the adsorbate (mg.L^{-1}), K_F is the Freundlich constant and n is the heterogeneity factor.

The linear form of Dubinin-Radushkevich (D-R) isotherm is expressed as [29]:

$$q_e = q_D \times e^{(-B_D \times [RT \ln(1 + \frac{1}{C_e})]^2)} \quad (9)$$

Where q_{max} (mg.g^{-1}) is the D-R isotherm constant related to the degree of adsorbate adsorption by the adsorbent surface, q_e is the amount adsorbed at equilibrium (mg.g^{-1}), B_D is related to the free energy of adsorption per mole of the adsorbate as it migrates to the surface of the adsorbent from infinite distance in the solution ($\text{mol}^2.\text{kJ}^{-2}$), T (K) is the temperature and C_e (mg.L^{-1}) is the equilibrium concentration of DB 79 at solution. The linearized form of the D-R equation is given in equation (10):

$$\ln q_e = \ln q_{max} - B_D \varepsilon^2 \quad (10)$$

$$\varepsilon = RT \ln(1 + \frac{1}{C_e}) \quad (11)$$

The apparent energy E of adsorption from Dubinin-Radushkevich is

$$E = \frac{1}{\sqrt{(2B_D)}} \quad (12)$$

The value of the apparent energy E between 8 and 16 kJ.mol^{-1} indicates a chemisorption process, but the values of E below 8 kJ.mol^{-1} represented a physical adsorption process

The linear form of Temkin isotherm is expressed as [30]:

The isotherm constants are presented in Table 2. The value of E in the present study is found to be below 8 kJ.mol^{-1} (Table 2) corresponding to physical adsorption process.

Temkin isotherm was described by the following equation:

$$q_e = (RT/bT) \ln(ATC_e) \quad (13)$$

$$B = RT/bT \quad (14)$$



Global Journal of Engineering Science and Research Management

B is the Temkin constant related to heat of sorption (J.mol^{-1}), A is the Temkin isotherm constant (L.g^{-1}), R the gas constant ($8.314 \text{ J.mol}^{-1} \text{ K}^{-1}$), b is Temkin isotherm constant and T is the temperature (K).

The parameters for the four isotherm models with regression coefficients (R^2) are summarized in Table 2. The capacity of DB 79 adsorbed at equilibrium increased from 37,5 to 121,167 mg.g^{-1} ; 1,95 to 8,175 mg.g^{-1} and 2,819 to 10,95 for CHT, PG and NP respectively by increasing the initial dye concentrations from 20 to 100 mg.L^{-1} . It can be seen that the Langmuir model was evidently the most appropriate to describe the adsorption process for all adsorbents due to their high correlation coefficients relative to the ones obtained from Freundlich, temkin and Dubinin–Radushkevich models. This result indicating that the monolayer of DB 79 covers the CHT, PG and NP surfaces.

The data of equilibrium isotherms of DB 79 onto all adsorbents is poorly described by the Freundlich, Temkin and Dubinin–Radushkevich models, due to their low values of R^2 compared to other models.

Table 2: Langmuir, Freundlich, Temkin and Dubinin–Radushkevich adsorption isotherms constants, correlation coefficients and the adsorption capacities of CHT, PG and NP for DB 79.

Table 2 : Isotherm parameters for the adsorption of DB 79 onto CHT, PG and NP.

Adsorbent		CHT	PG	NP
Freundlich	$k_F(\text{mg.g}^{-1} (\text{L.g}^{-1})^{1/n})$	60.39	2.61	3.65
	N	5.181	2.525	3.322
	R^2	0.502	0.662	0.963
Langmuir	$k (\text{L.mg}^{-1})$	0.615	0.244	0.318
	$Q (\text{mg.g}^{-1})$	125	10	10.87
	R^2	0.994	0.95	0.973
	R_L	0.09	0.08	0.14
Dubinin–Radushkevich	$q_D (\text{mg.g}^{-1})$	120	8	8,00
	$B_D (\text{mol}^2 \text{ kJ}^{-2})$	0.0000002	0.0000006	0.0000001
	$E_D (\text{KJ.mol}^{-1})$	1.6	0.9	2.2
	R^2	0.682	0.713	0.933
Temkin	$A_T (\text{L.g}^{-1})$	119.902	4.163	11.986
	$b_t (\text{J.mol}^{-1})$	14.11	1.825	1.631
	R^2	0.572	0.795	0.951

Thermodynamic parameters

The thermodynamic parameters such as change in Gibbs free energy (ΔG°), enthalpy (ΔH°) and entropy (ΔS°) are calculated using the following equations [31]:

$$\Delta G^\circ = -RT \ln K_L \quad (15)$$

$$\text{and} \quad \ln K_L = -\frac{\Delta H^\circ}{RT} + \frac{\Delta S^\circ}{R} \quad (16)$$

Where R ($8.314 \text{ J mol}^{-1} \text{ K}^{-1}$) is the gas constant, T (K) is the absolute temperature, and $K_L (\text{L.mol}^{-1})$ is the Langmuir constant. The calculated constants are listed in Table 3, the values of ΔG° are negative, which indicates that the adsorption process is spontaneous. Moreover, the positive values of ΔH° show that the adsorption was endothermic for DB 79 onto PG and NP, but the negative value of ΔH° for CHT show that the adsorption was exothermic, the positive ΔS° values suggest the increasing randomness at the PG/ DB 79 and NP/DB 79 interface



during the adsorption processes [32], however the negative ΔS° value for CHT suggests a decrease in randomness at its CHT/DB 79 interface [33]

Table 3 : Thermodynamic parameters for the adsorption of DB 79 onto CHT, PG and NP.

Adsorbent	ΔG° KJ mol ⁻¹					ΔH° KJ mol ⁻¹	ΔS° KJ mol ⁻¹ K ⁻¹
	293	303	313	323	333		
CHT	-11.00	-6.86	-5.47	-4.41	-2.47	-68.11	-0.20
PG	-0.67	-1.31	-1.71	-2.39	-3.13	16.83	0.06
NP	-0.02	-0.23	-1.87	-2.77	-4.07	65.99	0.21

CONCLUSION

The results of this investigation show that CHT, PG and NP can efficiently remove DB 79 from aqueous solution. The adsorption equilibrium is attained within 60 min for CHT and PG and 180 min for NP. The adsorption kinetics were verified by pseudo-second-order model for all adsorbents. The equilibrium adsorption isotherms were described by the Langmuir model for CHT, PG and NP. Maximum adsorption reached 125 mg.g⁻¹, 10 mg.g⁻¹ and 10.87 mg.g⁻¹ for CHT, PG and NP respectively. The adsorption was found to be spontaneous for the three adsorbents, exothermic for CHT and endothermic for PG and NP according the thermodynamic parameters. The CHT, PG and NP can be used as low cost and abundant adsorbents for the removal of DB 79.

REFERENCES

1. T.H. Kim, C. Park, J. Yang, S. Kim, Comparison of disperse and reactive dye removals by chemical coagulation and Fenton oxidation, *J. Hazard. Mater.* B112 (2004) 95–103
2. M. Neamtu, A. Yediler, I. Siminiceanu, M. Macoveanu, A. Kettrup, Decolorization of disperse red 354 azo dye in water by several oxidation processes a comparative study, *Dyes Pigments* 60 (2004) 61–68
3. **Lataye D. H.**, Mishra, Indra M., Mall, Indra D. Removal of 4-Picoline from Aqueous Solution by Adsorption onto Bagasse Fly Ash and Rice Husk Ash: Equilibrium, Thermodynamic and Desorption Study. *ASCE: Journal of Environmental Engineering*, 137 [11] (2011) 1048-1057.
4. M. Muthukumar, N. Selvakumar, Studies on the effect of inorganic salts on decoloration of acid dye effluents by ozonation, *Dyes Pigments* 62 (2004) 221–228.
5. C. Allegre, M. Maisseu, F. Charbit, P. Moulin, Coagulation-flocculation decantation of dye house effluents: concentrated effluents, *J. Hazard. Mater.* B 116 (2004) 57–64.
6. G. Annadurai, R. S. Juang, D. J. Lee, Factorial design analysis for adsorption of dye on activated carbon beads incorporated with calcium alginate, *Adv. Environ. Res.*, 6(2002), 191-198
7. A. Ely, M. Baudu, M.O.S.A.O. Kankoub, J.P. Basly, Copper and nitrophenol removal by low cost alginate/Mauritanian clay composite beads, *Chem. Eng. J.* 178 (2011) 168–174
8. R.S. Juang, R.L. Tseng, F.C. Wu, S.H. Lee, Adsorption behavior of reactive dyes from aqueous solutions on chitosan, *J. Chem. Technol. Biotechnol.* 70 (1997) 391–399.
9. H.Y. Zhu, R. Jiang, Y.Q. Fu, J.H. Jiang, L. Xiao, G.M. Zeng, Preparation, characterization and dye adsorption properties of c-Fe₂O₃/SiO₂/chitosan composite, *Appl. Surf. Sci.* 258 (2011) 1337–1344.
10. A. Bennani Karim, B. Mounir, M. Hachkar, M. Bakasse, A. Yaacoubi, Removal of Basic Red 46 dye from aqueous solution by adsorption onto Moroccan clay, *Journal of Hazardous Materials* 168 (2009) 304–309
11. Vakili, M.; Rafatullah, M.; Salamatinia, B.; Abdullah, A.Z.; Ibrahim, M.H.; Tan, K.B.; Gholami, Z.; Amouzgar, P. Application of chitosan and its derivatives as adsorbents for dye removal from water and wastewater: A review. *Carbohydr. Polym.* 2014, 113, 115–130.
12. K.rida, B.chemmal, A.boukhemkhem, Removal of methylene blue from aqueous solution by natural phosphate, *journal of optoelectronics and advanced materials*, Vol. 13, No. 5-6, May - June 2013, p. 493 - 500
13. N. Balkaya, H. Cesur, Adsorption of cadmium from aqueous solution by phosphogypsum, *Chemical Engineering Journal* 140 (2008) 247–254



Global Journal of Engineering Science and Research Management

14. S.K.Katti, D.R.Katti, R.Dash, Synthesis and characterization of a novel chitosan/montmorillonite/hydroxyapatite nanocomposite for bone tissue engineering *Biomed. Mater.* **3** (2008) 034122 (12pp)
15. N. Balkaya, H. Cesur, Adsorption of cadmium from aqueous solution by phosphogypsum, *Chemical Engineering Journal* **140** (2008) 247–254
16. N. Barka, A. Assabbane, A/ Nounah, L/Laanab, Y.A.Ichou, Removal of textile dyes from aqueous solutions by natural phosphate as a new adsorbent, *Desalination* **235** (2009) 264–275
17. M.S. Pendekal, P.K. Tegginamat, Hybrid drug delivery system for oropharyngeal, cervical and colorectal cancer – in vitro and in vivo evaluation, *Saudi.Pharm.J.* **21**(2013)177–186.
18. I. Hammas, K. Horchani-Naifer, M. Férid, Solubility study and valorization of phosphogypsum salt solution, *International Journal of Mineral Processing* **123** (2013) 87–93.
19. L. EL GAINI, A. MEGHEA, M. BAKASSE, Phototransformation of pesticide in the presence of moroccan natural phosphate in aqueous solution, *journal of optoelectronics and advanced materials* Vol. **12**, No. 9, September 2010, p. 1981 – 1985
20. Z.A. Zakaria, M. Suratman, N. Mohammed, W.A. Ahmad, Chromium(VI) removal from aqueous solution by untreated rubber wood sawdust, *Desalination* **244** (2009) 109–121
21. G.Hallas, J.H.Choi, Synthesis and properties of novel aziridinyl azo dyes from 2- aminothiophenesdPart 2: Application of some disperses dyes to polyester fibres. *Dyes Pigments* **1999**; **9**:67e73
22. T.G. Venkatesha, R. Viswanatha, Y. Arthoba Nayaka , B.K. Chethana, Kinetics and thermodynamics of reactive and vat dyes adsorption on MgO nanoparticles, *Chemical Engineering Journal* **198–199** (2012) 1–10
23. Hai-song Zhu, Xiao-juan Yang, Yan-peng Mao, Yu Chen, Xiang-li Long, Wei-kang Yuan, Adsorption of EDTA on activated carbon from aqueous solutions, *Journal of Hazardous Materials* **185** (2011) 951–957
24. Y.S. Ho, G. McKay, A comparison of chemisorption kinetic models applied to pollutant removal on various sorbents, *Trans. IChemE.* **76B** (1998) 332–340.
25. M. Monier, D.M. Ayad, Y. Wei, A.A. Sarhan, Adsorption of Cu(II), Co(II), and Ni(II) ions by modified magnetic chitosan chelating resin, *J. Hazard. Mater.* **177** (2010) 962–970.
26. Langmuir, The adsorption of gases on plane surfaces of glass, mica and platinum, *J. Am. Chem. Soc.* **40** (1918) 1361–1403
27. Z.M. Ni, S.J. Xia, L.G. Wang, F.F. Xing, G.X. Pan, Treatment of methyl orange by calcined layered double hydroxides in aqueous solution: adsorption property and kinetic studies, *J. Colloid Interface Sci.* **316** (2007) 284–291
28. H.M.F. Freundlich, Uber die adsorption in losungen, *Z. Phys. Chem.* **57A** (1906) 385–470.
29. A. Gunay, E. Arslankaya, I. Tosun, Lead removal from aqueous solution by natural and pretreated clinoptilolite: adsorption equilibrium and kinetics, *J.Hazard. Mater.* **146** (2007) 362–371
30. M. Temkin, V. Pyzhev, Recent modifications to Langmuir isotherms, *Acta Physiochim. USSR* **12** (1940) 217–222
31. Y. Ren, H.A. Abbood, F. He, H. Peng, K. Huang, Magnetic EDTA-modified chitosan/SiO₂/Fe₃O₄ adsorbent: preparation, characterization, and application in heavy metal adsorption, *Chemical Engineering Journal* **226** (2013) 300–311.
32. X.J. Hu, J.S. Wang, Y.G. Liu, X. Li, G.M. Zeng, Z.L. Bao, X.X. Zeng, A.W. Chen, F. Long, Adsorption of chromium (VI) by ethylenediamine-modified cross-linked magnetic chitosan resin: isotherms, kinetics and thermodynamics, *J. Hazard. Mater.* **185** (2011) 306–314
33. M. Alkan, O. Demirbas, M. Dogan, Adsorption kinetics and thermodynamics of an anionic dye onto sepiolite, *Micropor. Mesopor. Mater.* **101** (2007) 388–396